Cathodoluminescence and photoluminescence of swift ion irradiation modified zinc oxide-porous silicon nanocomposite

Yogesh Kumar, Manuel Herrera, Fouran Singh, S.F. Olive-Méndez, D. Kanjilal, Shiv Kumar, V. Agarwal

Abstract

We report the room temperature cathodoluminescence and photoluminescence of swift ion irradiated (130 MeV Nickel ion) porous silicon zinc oxide nanocomposites. The evolution of a broad and flat emission band from 1.5 to 3.5 eV is demonstrated. Annealing effect of irradiation is found to result in a relative increase in the band edge emission. Emission wavelength can be tuned in the complete visible range by changing the substrate characteristics.

Keywords: Porous silicon, Zinc oxide, SHI irradiation, Cathodoluminescence, Photoluminescence.

Introduction

In the recent years, there has been a consistent effort to replace bulk materials to thin films due to their capability to minimize the size of different devices and to integrate themselves with the silicon technology. Due to the fact that zinc oxide is compatible with silicon based IC processes [1], its ease of fabricating good quality thin films by sputtering as well as its possible applications in gas sensors, UV resistive coating, piezoelectric devices [2,3], varistors, transparent conductive oxide electrode and light emitting devices, it has been widely investigated on various substrates [4,5], or porous templates [6,7]. Motivated by its compatibility with silicon based IC technology, studies

have been made on ZnO films grown on porous silicon (PS) templates as well [8–13]. PS has been considered as one of the important Si-based luminescent materials since Canham presented the first observation of efficient photoluminescence from porous Si at room temperature [14]. Its open structure and large surface area, combined with unique optical and electrical properties, makes it a good option for templates [15,16]. In general, the emission energy of porous Si layers increases with decreasing silicon crystallite size, covering the entire visible spectrum from red to blue [17,18] and the red-emitting PS can be obtained easily. If the red emission from porous Si layers could be combined with a blue–green emission from a ZnO film, it would be possible to obtain white light. This combination opens a possible route for a white LED, which is important for display technology. In 2007 and 2009, our group [19–21] reported the white luminescence from the nanocomposites of ZnO-PS deposited by solgel spin coating technique. The origin of the luminescence was discussed by developing a flat band energy diagram, suggesting the basis of electron tunneling between the interface of ZnO and PS through the siloxene structure formed at the interface of zinc oxide and PS. Recently, Kayahan [22] also reported the white luminescence from thin films of zinc oxide deposited onto the n-type macroPS surface by rf-sputtering. The broadband PL spectra were discussed using oxygen bonding model for the PS and the native defects model for ZnO. Apart from that, many groups [23–25] have reported the UV light emission from modified PS. In particular, couple of works by Qin et al. group [23] have reported UV emission from thermally oxidized PS with the peak wavelength of 340–370 nm and concluded that the luminescence centers in silicon oxide were responsible for UV emission from oxidized PS and SiO_2 powder. In another work, Mizuno et al. [24]

reported UV emission due to post anodized treatment of PS in ethanoic HF solution. Tomioka and Adachi [25] reported the PL emission at 3.3 eV with a FWHM of 0.1 eV attributed to the surface oxide produced using photoetching method for the fabrication of PS. In spite of all the above-mentioned works on white light and UV emission from modified PS structures, there has been no work reporting a simultaneous observation of UV and white light. As the swift heavy ion (SHI) irradiation is one of the techniques which can be used for the modification of the optical and physical properties [26], in this work, swift ions of 130 MeV Nickel ions were used for the modification of the optical (photoluminescence/cathodoluminescence) and physical properties (morphology) of the composite film. To the best of our knowledge, for the first time we report the room temperature white light emission with a relatively similar intensity from band-edge, blue and green emission components from the zinc oxide coated PS composite, through cathodoluminescence (CL) spectroscopy.

Experimental details

PS samples were fabricated by wet electrochemical etching [27] of boron doped (1 0 0), silicon wafers with resistivity in the range 0.8–1.2 ohm-cm. For making the PS substrates with two different pore dimensions and thickness, the anodization was carried out using the current density of 30 mA/cm^2 (PS30) and 65 mA/cm^2 (PS65), with the anodization time of 429 and 240 s, respectively. The electrolyte composed of an equal volumetric ratio of HF and ethanol. The resulting thickness of the samples was 8 μm (PS30) and 10 μm (PS65). After the fabrication, samples were rinsed by ethanol and dried using pentane [28]. For the deposition of ZnO film on PS substrates using RF magnetron sputtering, substrate temperature was kept to be 300 °C and the deposition

chamber was evacuated to a pressure of ~9 × 10^{-6} Torr by turbo molecular pump backed by scroll pump. The ZnO films were deposited in Argon atmosphere at a base pressure of ~9 × 10^{-3} Torr. RF power was kept to be 150 W and deposition was carried out for 30 min for these samples. After the deposition the samples named (ZPS30), (ZPS65) and were annealed at the rate of 20 °C/min upto 700 °C (optimized as per our previously reported work [19,20]) in argon environment for 1 h.

The annealed films were irradiated with 130 MeV Ni ions using 15 UD Pelletron Accelarator at Inter University Accelerator Centre (IUAC), New Delhi. The samples were mounted on a rectangular shaped ladder and were irradiated in high vacuum (HV) chamber. The focused ion beam of constant current of about # 1.5 pnA (particles nanoampere) was scanned over an area of 1 × 1 cm^2. The above samples were irradiated with a fluence of 1 × 10^{13} ions/cm^2. On the other hand, the nuclear stopping and electronic stopping power (estimated from Stopping and Range of Ions in Matter (SRIM) simulations [29]) is 0.044 keV/nm and 24.63 keV/nm, respectively. Hence, the changes in physical and optical properties are mainly due to electronic excitations induced by SHI. The photoluminescence (PL) properties were studied using Varian Fluoroscence spectrometer (Cary Eclipse) under the excitation by 325 nm photons using 500 W Xenon lamp. Cathodoluminescence (CL) spectroscopy was done using Jeol JSM 5300 scanning electron microscope using electron beam energy of 15 keV. CL measurements were performed at 100 and 300 K in the UV–vis spectral range using a Hamamatsu R928P photomultiplier. A SPEX 340-E computer controlled monochromator was used for the spectral analysis. The structural properties of PS and its composites were analyzed using high resolution field emission SEM (JSM-7401F).

Results and discussion

The top (Fig. 1(a) and (b)) and cross sectional (Fig. 1(c) and (d)) view of ZPS30 composite (before and after irradiation) just after annealing reveals the overall thickness of PS of approximately 8 μm along with ZnO layer of 450 nm on the top. A close investigation of the structure reveals the microporous (with the average pore size less than 5 nm and 20 nm for ZPS30 and ZPS65) morphology of the PS layer (well known in 0.8–1.2 ohm cm resistivity) and a welldefined interface. Similar analysis for ZPS65 gives the average pore size and thickness of approximately 17 nm and 10 μm, respectively. In order to check the morphological changes, secondary electron images (Fig. 1) were analyzed before (pristine) (a) and after irradiation (b). Fig. 1(c) shows the cross sectional view with thin oxide layer on the top of the PS layer supported by the magnified view of the ZnO layer shown in Fig. 1(d). Before irradiation, the films are observed to have a relatively homogeneous distribution of ZnO over the PS substrate. The irradiated film (Fig. 1b) shows apparent changes in the morphology (appears as irradiation induced dark patches), (fluence: 1×10^{13} ions/cm^2), Such change in the size and shape of the crystallites is attributed to the high density of electronic excitations induced by SHI irradiation under multiple ion impacts in the near surface region [30].

Room temperature PL spectrum of ZPS30 (before and after irradiation) is shown in Fig. 2 and reveals the presence of two dominating peaks centered at 3.17 and 1.7 eV, before irradiation. The PL peak around 3.17 eV could be attributed to the excitonic emission of ZnO [31] and the emission band at 1.7 eV is due to PS [10]. A relatively small contribution of different defects (emission in the green blue region in the range 2.2–3.0 eV) in the zinc oxide layer has also been observed. In ZnO, usually two peaks

are most common: (a) a narrow UV emission at around 3.26 eV, due to exciton emission and (b) a broader emission band located in the green part of the visible spectrum. The presence of the green emission has been the subject of investigation [32–39] for the last many years and many hypotheses have been proposed for this emission [32–34]. Initially researchers suggested oxygen vacancies as the source of green emission in ZnO [35–37]. Recently it has been investigated that more than one deep levels are involved in the green emission in ZnO, i.e. VO (oxygen vacancy) and V_{Zn} (zinc vacancies) [33,38,39]. Therefore, in conformity to the above-mentioned literature, green emission can be attributed to the presence of oxygen vacancies.

After irradiation, the emission corresponding to ZPS30 reveals the evolution of the broad peak in the visible region which can be deconvoluted into three peaks, centered at around 1.7, 2.7 and 3.16 eV. The peak around 2.7 eV can be attributed to the transitions generated by amorphous SiO_x formed on PS [40], although some works have also attributed such peaks to the transitions between Zn_i states and V_{Zn}/conduction band to V_{Zn} or oxygen vacancies (V_0) [41,42]. The peak intensity corresponding to 2.7 eV (after irradiation) has been found to increase by a factor of 10 with respect to the pristine sample, where the presence of defects is almost insignificant. On the other hand, the relative peak intensity corresponding to excitonic emission (3.16 eV) was observed to increase by a factor of 3 (Fig. 2; black line). The peak at 1.70 eV corresponding to PS has been found to decrease significantly in accordance with the results reported previously by Wolkin et al. [17]. In order to understand the contribution and the evolution of the defect related PL results, CL measurements were taken before and after the irradiation at 100 and 300 K. Fig. 3

shows CL spectra from sample ZPS30 acquired before and after the irradiation with a broad band white light emission from 1.75 to 4.0 V generated from the ZnO film and PS. CL spectra reveals some similarity with the PL spectra (discussed above) with an exception of the evolution of the UV emission peak. The CL spectra acquired at 100 K (Fig. 3(a) and (b)) show several well defined shoulders that permitted a deconvolution using Gaussian curves to find four components centered at 2.0, 2.68, 3.24 and 3.8 eV. Similar to the PL spectra, the CL component at 3.24 eV is assigned to the ZnO band edge emission and the component at 2.0 eV is the well-known ZnO-defect related yellow band [43,44]. As mentioned before during the PL discussion, the UV and blue components of 3.8 and 2.68 eV, have been previously reported by Arakaki et al. [40] and have been attributed to the amorphous SiO_x formed on PS.

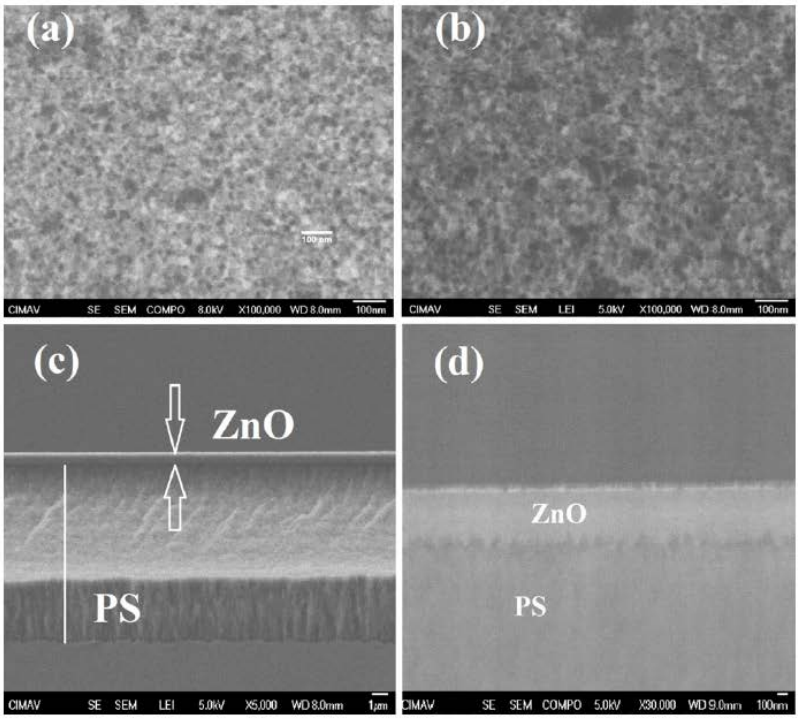

Fig. 1. SEM images of pristine ZnO/PS film after annealing at 700 °C for 1 h, showing the top and the cross-sectional view with ZnO layer at the top. (a) ZPS 30 before irradiation. (b) ZPS 30 after irradiation at fluence 1×10^{13} ions/cm^2. (c) ZnO thin film over the PS layer of almost 8 μm (d) a closer view of the zinc oxide layer and the PS–ZnO interface.

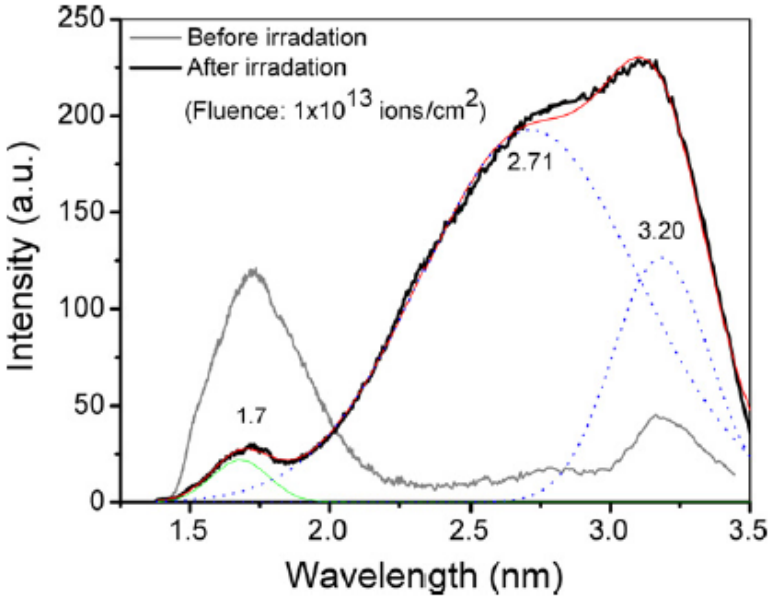

Fig. 2. PL spectra of ZPS30 before (grey line) and after irradiation (black line) with 130 MeV Nickel ions at fluence 1×10^{13} ions/cm^2; dotted lines show the de-convoluted components of the sample ZPS30 after irradiation.

The formation of oxygen vacancies and impurities in the oxidized silicon has been proposed previously as the origin of these two bands [45,46]. However, the formation of an intense blue band centered at 2.78 eV has been reported more recently by Zhang et al. in ZnO films grown on SiO_2 substrates (Corning 7059) [47], and was assigned to electron transitions from shallow levels, generated by oxygen vacancies or interstitial zinc, to valence band. Moreover, this blue band has also been found in ZnO–SiO_2 nanocomposites [48,49] and their origin has been attributed to point defects generated at the ZnO/SiO_2 interface [50]. Recently it has been demonstrated that blue emission is also produced by ZnO nanostructures, without an interface ZnO/SiO_2 [51,52] apparently generated due oxygen vacancies or interstitial zinc. The formation of point defects associated to this blue band in the ZnO film and at the interface ZnO/SiO_2, generated onto PS, could explain the behavior of this emission in our samples.

Particularly, the CL measurements recorded more clearly the presence of this emission from the non-irradiated sample than PL measurements (Figs. 3(a) and 2(a) respectively), apparently due to the higher penetration of the electron beam, which excited the radiative-centers present at the interface ZnO/SiO_2/PS. The high sensibility of the CL technique to recorded emissions generated by point defects or impurities in semiconductors could explain this behavior [53,54]. The CL spectra acquired at 300 K before and after the irradiation recorded a broad emission centered at 2.5 and 2.3 eV, respectively (Fig. 3(c) and (d)), which were deconvoluted for the ZnO bands at about 2.18, 2.7 and 3.2 eV. As compared to the CL results acquired at 100 K, at room temperature the intensity of UV emission is low. In contrast to the PL measurements, CL spectra taken at 300 K shows that after irradiation the relative intensity of the blue band decreased in intensity. As has been commented, the difference in the relative intensity to this emission in PL and CL spectra is assigned to the different regions excited in sample, using electromagnetic waves (PL) or the electron beam (CL). These complementary results suggest that irradiation generates point defects (associated with the blue band) on the surface of the film and an annealing at the interface ZnO/SiO_2/PS. The penetration depth of the ions used in the irradiation was upto 9 μm.

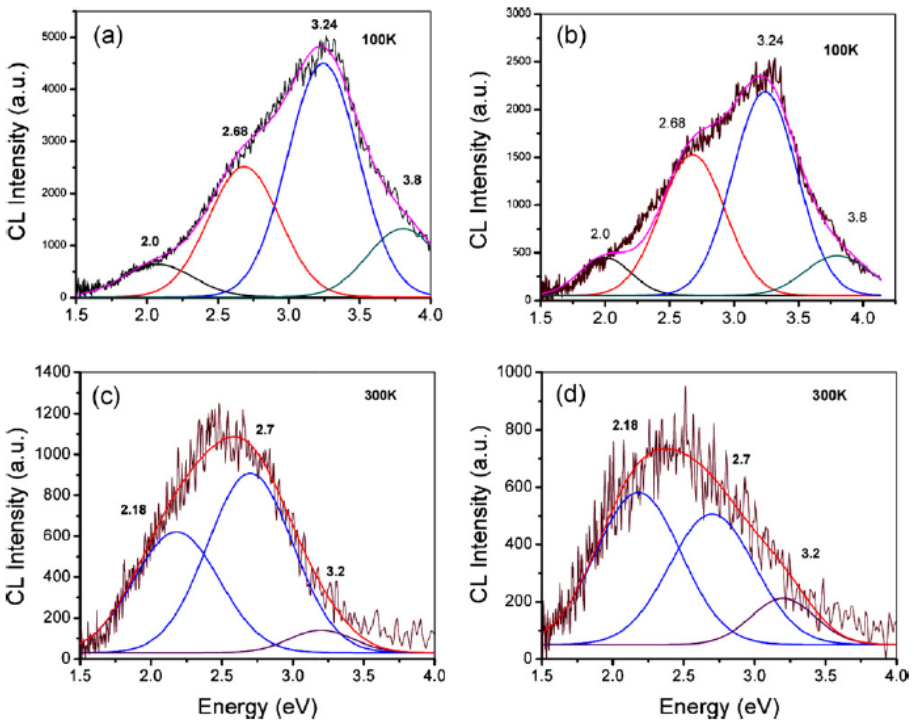

Fig. 3. Cathodoluminescence spectra of sample ZPS 30 at 100 and 300 K (a) and (c) before irradiation and (b) and (d) after irradiation.

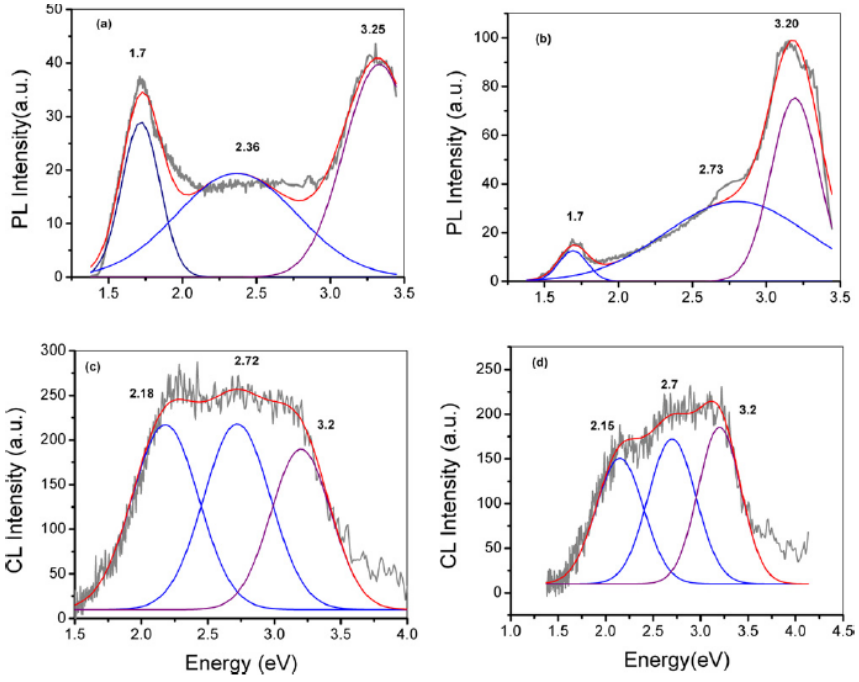

Fig. 4. Emission spectra of sample ZPS 65 at 300 K (a) PL spectra (pristine) (b) PL spectra after irradiation and (c) cathodoluminescence spectra (Pristine) (d) CL after irradiation.

Additionally, the ratio of the intensities (I_{band}-edge/I_{blue}) measured before and after irradiation were 0.12 and 0.35 at 300 K, respectively, which revealed a decrease in the relative intensity of the blue band accompanied with an increase in the relative intensity of the band edge emission after irradiation. Since the yellow emission is shown to retain the emission intensity constant after the irradiation (at about 600 a.u.), this increase of the band-edge emission could be explained in terms of an increase in the number of transitions between the conduction and valence bands, due to a decrease in the number of electronic levels associated to the blue emission. On the other hand, the values of this ratio, $I_{band\text{-}edge}/I_{blue}$, measured at 100 K, calculated as 1.97 and 1.50, before and after the irradiation, respectively, reveal an increase in the blue emission after irradiation. As commented before, CL measurements reveal the emission originated at the interface ZnO/SiO_2/PS, and to the difference in temperature (300–100 K) a variation in the strain between the ZnO film and the SiO_2/PS substrate is expected. Due to the high thermal expansions of the PS [55], a large strain in the ZnO film is expected at 100 K, which could generate the point defects associated with the blue emission at the interface.

PL spectra from sample ZPS65 before irradiation, acquired at 300 K (Fig. 4(a)), recorded the red band (1.71 eV) of the PS, a flat and broad emission between 2 and 3 eV, and the band edge (3.25 eV) of the ZnO. After irradiation, the sample recorded a strong increase in the band edge emission with a decrease in the intensity of the PS band (Fig. 4(b)). CL spectra acquired at same temperature from the non irradiated sample shows a broad and flat emission between 1.5 and 3.5 eV (Fig. 4(c)), which was deconvoluted with components corresponding to the yellow (2.18 eV), blue (2.7 eV) and

band edge (3.2) emissions of the ZnO. As has been commented, the sensibility of the CL technique to detect the defect related emissions in these samples is attributed to the excitation of the radiative centers at the interface ZnO/SiO_2/PS. After irradiation, a decrease in the intensity of the yellow and blue emissions was recorded in CL spectra (Fig. 4 (d)), apparently due to an annealing effect, analogous with the results obtained with sample ZPS30.

Analysing the PL spectra of both the samples, the relative contribution due to PS was decreased to 25% and 50% of its original luminescence for the sample ZPS 30 (Fig. 2) and ZPS 65 (Fig. 4(a) and (b)), respectively. The sample ZPS30 (made with the relatively small pore size substrate) shows a significant increase of defects as compared to ZPS 65. The relative changes in the emission peaks in sample ZPS 30 are more pronounced than ZPS65. Hence, the optical properties of the composites studied in this work change significantly with the change in the substrate characteristics and are found to be tunable in the complete visible range.

Conclusion

Simultaneous observation of white light and UV emission has been reported on the zinc oxide-PS nanocomposite through Cathodoluminescence spectroscopy. The two luminescence measurement techniques have been found to complement each other and CL is found to provide more information on the defects related luminescence. Although, defects have been shown to increase after modifying the structure through irradiation, annealing effects of SHI irradiation are revealed. Change in the substrate characteristics is found to tune the room temperature emission spectra of the deposited ZnO film.

Acknowledgments

Authors are also thankful to DST, Govt. of India and CONACyT, Mexico for providing the bilateral exchange project (DST/INT/MEX/RPO-09/2008 and Mexico-India J000.0374). The author (VA) also acknowledges the partial support given by CONACyT project number 128593. MHZ acknowledges the support of the project CONACyT 102519. The author (YK) acknowledges the CONACyT support (179496) for doctoral scholarship. We acknowledge the technical support provided by M.C. Enrique Torres for doing the XRD and Wilber Antunez for SEM at CIMAVChihuahua.

References

[1] M.J. Vellekoop, C.C.G. Visser, P.M. Sarro, A. Venema, Sensors and Actuat A. Phys. 23 (1990) 1027–1030.

[2] R.P. Ried, E. Kim, D.M. Hong, R.S. Muller, J. Microelectromech. Syst. 2 (1993) 111–120.

[3] Y. Ito, K. Kushida, K. Sugawara, H. Takeuchi, IEEE Trans. Ultrason., Ferroelectrics, Freq. Contr. 42 (1995) 316–324.

[4] H.J Ko, Y.F. Chen, Z. Zhu, T. Yao, I. Kobayashi, H. Uchiki, Appl. Phys. Lett. 76 (2000) 1905–1907.

[5] A. Ohtomo, K. Tamura, K. Saikusa, T. Takahashi, T. Makino, Y. Segawa, H. Koinuma, M. Kawasaki, Appl. Phys. Lett. 75 (1999) 2635–2637.

[6] W.H. Zhang, J.L. Shi, L.Z. Wang, D.S. Yan, Chem. Mater. 12 (2000) 1408–1413.

[7] Y. Li, G.W. Meng, L.D. Zhang, F. Phillipp, Appl. Phys. Lett. 76 (2000) 2011–2013.

[8] Y.L. Liu, Y.C. Liu, H. Yang, W.B. Wang, J.G. Ma, J.Y. Zhang, Y.M. Lu, D.Z. Shen, X.W. Fan, J. Phys. D: Appl. Phys. 36 (2003) 2705–2708.

[9] S.Q. Chen, J. Zhang, X. Feng, X.H. Wang, L.Q. Luo, Y.L. Shi, Q.S. Xue, C. Wang, J.Z. Zhu, Z.Q. Zhu, Appl. Surf. Sci. 241 (2005) 384–391.

[10] B. Zhao, L.Q. Shan, Q.H. Sia, N. Zhang, Chin. Phys. Lett. 23 (2006) 1299–1301.

[11] G.Hu. S.Q. Li, H. Gong, Y. Zhao, J. Zhang, T.L. Sudesh, L. Wijesinghe, D.J. Blackwood, J. Phys Chem. C 113 (2009) 751–754.

[12] K. Yu, Y. Zhang, L. Luo, W. Wang, Z. Zhu, J. Wang, Y. Cui, H. Ma, W. Lu, Appl. Phys. A 79 (2004) 443–446.

[13] R. Prabakaran, T. Monteiro, M. Peres, A.S. Viana, A.F. Da Cunha, H. Aguas, A. Goncalves, E. Fortunato, R. Martins, I. Ferreira, Thin Solid Films 515 (2007) 8664–8669.

[14] L.T. Canham, Appl. Phys. Lett. 57 (1990) 1047–1049.

[15] D. Xu, G. Guo, L. Gui, Y. Tang, Z. Shi, Z. Jin, Z. Gu, W. Liu, X. Li, G. Zhang, Appl. Phys. Lett. 75 (1999) 481–483.

[16] V. Chin, B.E. Collins, M.J. Sailor, S.N. Bhatia, Adv. Mater. 13 (2001) 1877–1880.

[17] M.V. Wolkin, J. Jorne, P.M. Fauchet, G. Allan, C. Delerue, Phys. Rev. Lett. 82 (1999) 197–200.

[18] X.L. Wu, S.J. Xiong, D.L. Fan, Y. Gu, X.M. Bao, G.G. Siu, M.J. Stokes, Phys. Rev. B 62 (2000) R7759–R7762.

[19] R.G. Singh, F. Singh, V. Agarwal, R.M. Mehra, J. Phys. D: Appl. Phys. 40 (2007) 3090–3093.

[20] R.G. Singh, F. Singh, D. kanjilal, V. Agarwal, R.M. Mehra, J. Phys. D: Appl. Phys. 42 (2009) 062002.

[21] R.G. Singh, F. Singh, I. Sulania, D. Kanjilal, K. Sehrawat, V. Agarwal, R.M. Mehra, Nucl Instrum. Methods Phys. Res. Sect. B 267 (2009) 2399–2402.

[22] E. Kayahan, J. Lumin. 130 (2010) 1295–1299.

[23] G.G. Qin, J. Lin, J.Q. Duan, G.Q. Yao, Appl. Phys. Lett. 69 (1996) 1689–1691.

[24] H. Mizuno, H. Koyama, N. Koshida, Appl. Phys. Lett. 69 (1996) 3779–3781.

[25] K. Tomioka, S. Adachi, Appl. Phys. Lett. 87 (2005) 251920.

[26] A. Berthelot, F. Gourbilleau, C. Dufour, B. Domenges, E. Paumier, Nucl. Instrum. Methods Phys. Res. Sect. B 166 (2000) 927–932.

[27] V. Agarwal, J.A. Del Rio, Appl. Phys. Lett. 82 (2003) 1512–1514.

[28] O. Belmont, D. Bellet, Y. Brechet, J. Appl. Phys. 79 (1996) 7586–7591.

[29] J.F. Ziegler, P. Biersack, U. Littmark, Stopping and Ranges of Ions in Matter,

Pergamon, New York, 1985.

[30] S. Hémon, A. Berthelot, C. Dufour, F. Gourbilleau, E. Dooryhée, S.B. Colin, E. Paumier, Eur. Phys. J. B 19 (2001) 517–524; D.C. Agarwal, F. Singh, D. Kabiraj, S. Sen, P.K. Kulariya, I. Sulania, S. Nozaki, R.S. Chauhan, D.K. Avasthi, J. Phys. D: Appl. Phys. 41 (2008) 045305.

[31] X.L. Wu, G.G. Siu, C.L. Fu, H.C. Ong, Appl. Phys. Lett. 78 (2001) 2285–2287.

[32] A.B. Djurisic, Y.H. Leung, Small 2 (2006) 944–961.

[33] Q.X. Zhao, P. Klason, M. Willander, H.M. Zhong, W. Lu, J.H. Yang, Appl. Phys. Lett. 87 (2005) 211912.

[34] K. Vanheusden, C.H. Seager, W.L. Warren, D.R. Tallant, J.A. Voigt, Appl. Phys. Lett. 68 (1996) 403–405.

[35] F.A. Kroger, H.J. Vink, J. Chem. Phys. 22 (1954) 250–252.

[36] P.H. Kassai, Phys. Rev. 130 (1963) 989–995.

[37] S.A. Studenikin, N. Golego, M. Cocivera, J. Appl. Phys. 84 (1998) 2287–2294.

[38] T.M. Borseth, B.G. Svensson, A.Y. Kuznetsov, P. Klason, Q.X. Zhao, M. Willander, Appl. Phys. Lett. 89 (2006) 262112.

[39] P. Klason, T.M. Borseth, Q.X. Zhao, B.G. Svensson, A.Y. Kuznetsov, M. Willander, Sol. Stat. Commun. 145 (2008) 321–326.

[40] O. Arakaki, A. Hatta, T. Ito, A. Kiraki, Jpn J. Appl. Phys. 33 (1994) 6586–6590.

[41] C.H. Ahn, Y.Y. Kim, D.C. Kim, S.K. Mohanta, H.K. Cho, J. Appl. Phys. 105 (2009) 013502.

[42] Z. Fang, Y. Wang, D. Xu, Y. Tan, S. Liu, Opt. Mater. 26 (2004) 239–242.

[43] M.A. Reshchikov, J.Q. Xie, B. Hertog, A. Osinsky, J. Appl. Phys. 103 (2008) 103514; A. González, M. Herrera, J. Valenzuela, A. Escobedo, U. Pal, Superlattice and Microst. 45 (2009) 421–428.

[44] M.A. Reshchikov, J.Q. Xie, B. Hertog, A. Osinsky, J. Appl. Phys. 103 (2008) 103514.

[45] H. Koyama, J. Appl. Phys. 51 (1980) 2228–2235.

[46] S.W. McKnight, E.D. Palik, J. Non-Cryst. Solids 40 (1980) 595–603.

[47] D.H. Zhang, Z.Y. Xue, Q.P. Wang, J. Phys D: Appl Phys. 35 (2002) 2837–2840.

[48] H. He, Y. Wang, Y. Zou, J. Phys. D: Appl. Phys. 36 (2003) 2972–2975.

[49] M. Abdullah, S. Shibamoto, K. Okuyama, Opt. Mater. 26 (2004) 95–100.

[50] Y.Y. Peng, H.T. Eong, H.C. Hsu, Nanotechnology 17 (2006) 174–181.

[51] W. Cheng, P. Wu, X. Zou, T. Xiao, J. Appl. Phys. 100 (2006) 054311.

[52] H. Zeng, Z. Li, W. Cai, P. Liu, J. Appl. Phys. 102 (2007) 104307.

[53] J. Piqueras, D. Maestre, Y. Ortega, A. Cremades, P. Fernández, Scanning 30 (2008) 354–357.

[54] M. Herrera-Zaldívar, P. Fernández, J. Piqueras, J. Solis, J. Appl. Phys. 85 (1999) 1120–1123.

[55] C. Faivre, D. Bellet, G. Dolino, J. Appl. Phys. 87 (2000) 2131–2136.